ARTICLE

Hyaluronan biopolymers release water upon pH-induced gelation

Eliane P. van Dam,* Giulia Giubertoni, Federica Burla, Gijsje H. Koenderink and Huib J. Bakker [a]

Received 00th January 20xx,
Accepted 00th January 20xx

DOI: 10.1039/x0xx00000x

We study the relation between the macroscopic viscoelastic properties of aqueous hyaluronan polymer solutions and the molecular-scale dynamics of water using rheology measurements, differential dynamic microscopy, and polarization-resolved infrared pump-probe spectroscopy. We observe that the addition of hyaluronan to water leads to a slowing down of the reorientation of a fraction of the water molecules. Near pH 2.4, the viscosity of the hyaluronan solution reaches a maximum, while the number of slowed down water molecules reaches a minimum. This implies that the water molecules become on average more mobile when the solution becomes more viscous. This observation indicates that the increase in viscosity involves the expulsion of hydration water from the surfaces of the hyaluronan polymers, and a bundling of the hyaluronan polymer chains.

Introduction

Hyaluronan is a biopolymer that is present in many biological tissues and fluids, including cartilage and synovial fluid.[1,2] Hyaluronan is composed of repeating D-glucuronic acid and N-acetyl-D-glucosamine disaccharide units (see Figure 2B inset), and is found in nature in a large range of sizes (from oligosaccharides to millions of Daltons). Hyaluronan is involved in a wide range of biological functions, including skin hydration and joint lubrication,[3–5] cancer progression and metastasis[6,7] and regulation of cell behaviour.[7,8] Its unique properties are to a large extent thought to be linked to its high water-binding capacity (the ability to hold water during centrifugation[9,10]). This water-binding capacity was found to be the largest in a quite narrow pH range around pH 2.4, where solutions of hyaluronan turn into an elastic gel referred to as a putty state.[11]

The origin of the sol-gel transition at pH=2.4 was extensively studied by measuring the rheology.[11–15] It was hypothesized that near pH 2.5, interchain hydrogen bonds are formed between the carboxylic acid and acetamide groups, thereby forming a high density of crosslinks leading to the formation of a putty state.[12,13] This hypothesis, was recently confirmed by two-dimensional femtosecond infrared spectroscopy.[16] In this paper, we study the fate of the water molecules in aqueous hyaluronan solutions during pH-induced changes in macroscopic viscoelastic properties, using a combination of rheology measurements, differential dynamic microscopy, and polarization resolved femtosecond infrared pump-probe spectroscopy.

[a] AMOLF, Science Park 104, 1098 XG Amsterdam, The Netherlands. E-mail: E.v.Dam@amolf.nl

Electronic Supplementary Information (ESI) available: experimental methods, $HClO_4$ measurements and pK_a determination. See DOI: 10.1039/x0xx00000x

Experimental

We perform an infrared pump-probe experiment in which we excite the OD stretch vibrations of HDO molecules with an intense laser pulse centered at 2500 cm^{-1}.[17] The resulting absorption changes $\Delta\alpha$ are probed with a second, weaker probe pulse, also centered at 2500 cm^{-1}. The probe pulse is polarized either parallel or perpendicular with respect to the polarization of the pump pulse. Directly after the excitation, at short delay times between pump and probe pulses, the measured absorption change will be larger in the parallel direction ($\Delta\alpha_{\parallel}$(v,t)) than in the perpendicular direction ($\Delta\alpha_{\perp}$(v,t)), because the vibrations that are oriented parallel to the polarization of the pump pulse will be excited most efficiently by the pump pulse. At longer delay times, the parallel and perpendicular signals will become equal due to reorientation of the HDO molecules. From the parallel and perpendicular signals we construct the reorientation independent isotropic signal:

$$\Delta\alpha_{iso}(\nu,t) = \frac{1}{3}(\Delta\alpha_{\parallel}(\nu,t) + 2\Delta\alpha_{\perp}(\nu,t)),$$

which decays with the vibrational lifetime. After correcting for the ingrowing heating signal,[17] we construct the vibrational relaxation independent anisotropy R:

$$R(\nu,t) = \frac{\Delta\alpha_{\parallel}(\nu,t) - \Delta\alpha_{\perp}(\nu,t)}{\Delta\alpha_{\parallel}(\nu,t) + 2\Delta\alpha_{\perp}(\nu,t)}$$

The anisotropy parameter *R(ν,t)* decays because of the reorientation of the HDO molecules.

We study the influence of the gelation of hyaluronan on the dynamics of the surrounding water molecules for two different sizes of hyaluronan: high molecular weight (1.5–1.8 MDa) and low molecular weight (100-150 kDa) hyaluronan. A detailed description of the experiment is given in the supporting information.

Results and Discussion

In Figure 1A we show the isotropic transient absorption spectra measured in the frequency region of the OD stretch vibration of HDO at different pump-probe delay times for a solution of 20 mg/ml high-molecular weight hyaluronic acid and 60 mM $HClO_4$ in isotopically diluted water. The isotropic spectra show a ground-state bleach at short time delays, and a thermal difference spectrum at long time delays. To extract the anisotropy of the excited OD stretch vibration, we subtract the heating contribution by fitting the spectra to a kinetic model that accounts for the vibrational relaxation and the rise of the heating contribution[17–19]. The result of this fit is shown as solid lines in Figure 1A. Figure 1B shows the resulting anisotropy of the OD stretch vibration as function of frequency, for different delay times. These results show that the anisotropy decay is frequency independent.

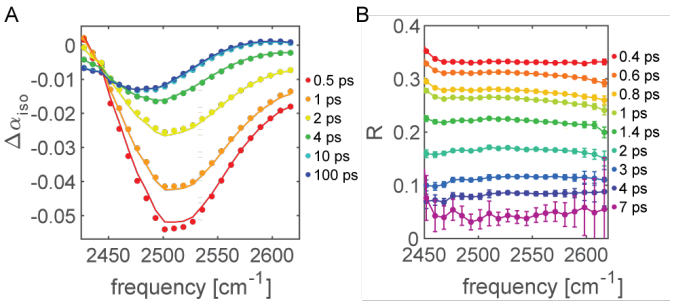

Figure 1. (A) Isotropic transient absorption change of the OD stretch vibration of HDO molecules for a solution of 20 mg/ml high-molecular weight hyaluronic acid and 60 mM $HClO_4$ in isotopically diluted water, for different picosecond delay times. The solid lines results from a fit to the model described in the text. (B) Anisotropy as a function of frequency for a solution of 20 mg/ml high-molecular weight hyaluronic acid and 60 mM $HClO_4$ in isotopically diluted water, for different picosecond delay times.

Figure 2 shows the anisotropy decay of solutions of hyaluronan at different $HClO_4$ concentrations in isotopically diluted water. For solutions of hyaluronan we observe that the anisotropy decay contains an additional slow component. We fit this anisotropy with an exponential decay with an offset, $R = R_0 e^{-t/\tau_r} + R_{slow}$. We find a time constant τ_r of 2.2±0.1 ps for all hyaluronic acid solutions, similar to the reorientation time constant of neat liquid water.[17] This exponentially decaying reorientation component thus represents water molecules for which the reorientation is not influenced by the presence of the hyaluronan polymer chains. The offset R_{slow} is attributed to water molecules for which the reorientation is strongly slowed down due to the interaction with hyaluronan polymer chains or with the other ions present in the solution.[20]

In Figure 3 we show the normalized offset, $R_{slow}/(R_{slow} + R_0)$ as a function of $HClO_4$ concentration (red points). We observe a decrease in the normalized offset of hyaluronan solutions with increasing concentration until 44 mM $HClO_4$, followed by an increase in offset until 60 mM $HClO_4$, and then again a decrease in offset. We also measured the anisotropy for a solution only containing ions (no hyaluronan), in order to distinguish between the fraction of slow water molecules resulting from the interaction with hyaluronan and the fraction of slow water

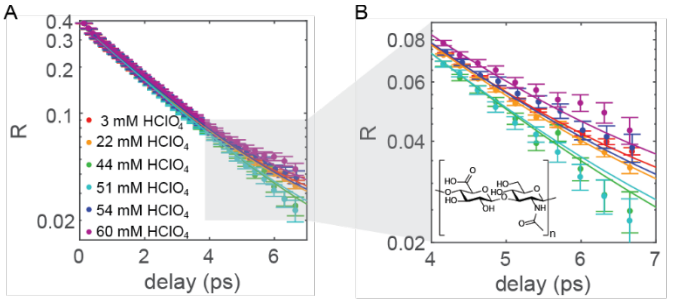

Figure 2. (A) Anisotropy decay as a function of delay time for solutions with 20 mg/ml high-molecular weight hyaluronan and different $HClO_4$ concentration in isotopically diluted water, averaged over the frequency range 2450-2550 cm^{-1}. The solid lines are fits to an exponential function with an offset. (B) Zoom-in of the anisotropy decay at delay times >4 ps. The inset shows the molecular structure of hyaluronan.

molecules resulting from the interaction with the ions. The result of these measurements (solutions of 150 mM NaCl and a varying concentration of $HClO_4$) are also shown in Figure 3 (blue). For the solutions that only contain ions, the fraction of slow water molecules increases linearly with the concentration of $HClO_4$. Comparison of the red and blue points shows that at most concentrations the hyaluronan has a much stronger slowing down effect than the ions.

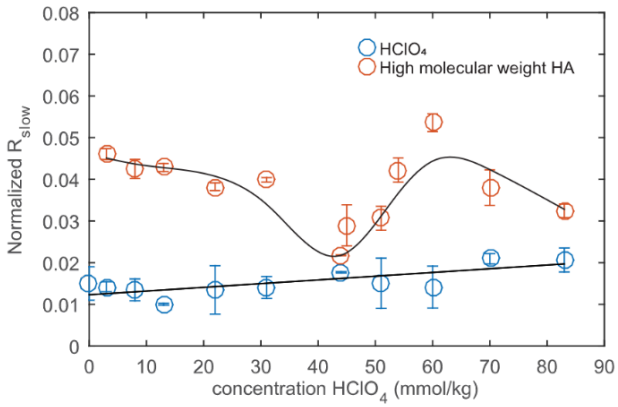

Figure 3. Normalized offset R_{slow} of the anisotropy decay as a function of $HClO_4$ concentration of solutions containing $HClO_4$, high molecular weight hyaluronan and 150 mM NaCl (red), and only containing $HClO_4$ and 150 mM NaCl (blue). All solutions are in isotopically diluted water. The solid lines are guides to the eye.

Figure 4 shows the anisotropy decay for solutions of low-molecular weight hyaluronan in isotopically diluted water. The data in this figure are analyzed in the same way as the data in Figure 2, i.e. fitted with an exponential decay and an offset. We observe that the offsets behave quite similarly as was observed for high-molecular weight hyaluronan, in spite of the fact that low-molecular weight hyaluronan does not form an elastic putty state near pH 2.4.[21,22]

As shown in Figure 5, the normalized offset R_{slow} shows a similar dependence on the $HClO_4$ concentration as for high-molecular

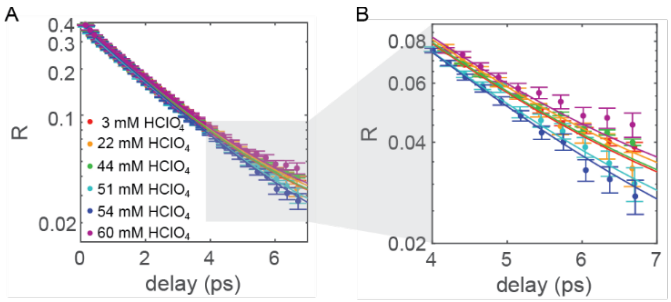

Figure 4. (A) Anisotropy decay as a function of delay time for solutions of low molecular weight hyaluronan with different $HClO_4$ concentration in isotopically diluted water and neat isotopically diluted water, averaged over the frequency range 2450-2550 cm^{-1}. The solid lines are fits to an exponential function with an offset. (B) Detail of the anisotropy decay.

weight hyaluronan, reaching a minimum at an $HClO_4$ concentration of 54 mM.

The dynamics of the anisotropy of the OD stretch vibration represents the reorientation of the water hydroxyl groups. The value of R_{slow} represents the fraction of water hydroxyl groups that are slowed down due to their interaction with hyaluronan and the ions present in solution. To determine the fraction of water hydroxyl groups that are slowed down because they are bound to hyalruonan, we first corrected the offset R_{slow} for the contribution of water molecules interacting with Na^+,Cl^- , H^+ and ClO_4^- by subtraction (see supplementary information). Subsequently, we calculated the number of slowly reorienting water hydroxyl groups N_{slow} per disaccharide unit of the hyaluronan polymer using the following expression:

$$N_{slow} = \frac{R_{slow}/(R_{slow}+R_0)}{c} \cdot 110.5,$$

where c represents the molar concentration of disaccharide units, and 110.5 is the number of moles of water hydroxyl groups contained in 1 liter. The resulting numbers of slowly reorienting hydroxyl groups per disaccharide unit of the hyaluronan chain are reported in Figure 6A and B for low and high molecular weight hyaluronan, respectively.

For the low-molecular weight variant, we observe an increase of the number of slow OH groups per disaccharide unit when the pH is increased up to pH 1.9. Then the number of slow OH groups sharply decreases, from 61±10 at pH 1.9 to 25±2 at pH=2.1. When the pH is further

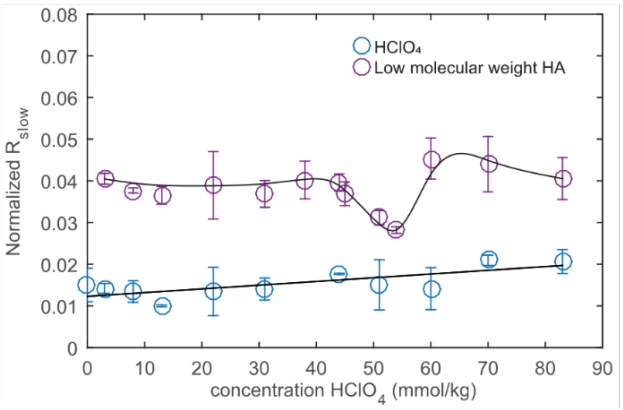

Figure 5. Normalized offset R_{slow} of the anisotropy decay as a function of HClO4 concentration of solutions containing $HClO_4$, low molecular weight hyaluronan and 150 mM NaCl (red), and only containing HClO4 and 150 mM NaCl (blue). All solutions are in isotopically diluted water. The solid lines are guides to the eye.

increased to 3, the number of slow groups increases again to 55±12, and stays more or less constant when the pH is further increased. For high-molecular weight hyaluronan, we observe 28±4 slow water OH groups per disaccharide unit at pH 1.5. This number increases with increasing pH to 79±5 slow OH groups at pH 1.9. After pH 1.9, the number of slow OH groups sharply decreases, to a minimum of 12±1 OH groups at pH 2.5. When the pH is further increased, the number of slow OH groups increases again. In Figure 6C we show the viscous and elastic shear moduli of the high-molecular weight hyaluronan solution (10 mg/ml) as a function of the pH. At pH 2.4, a sharp increase

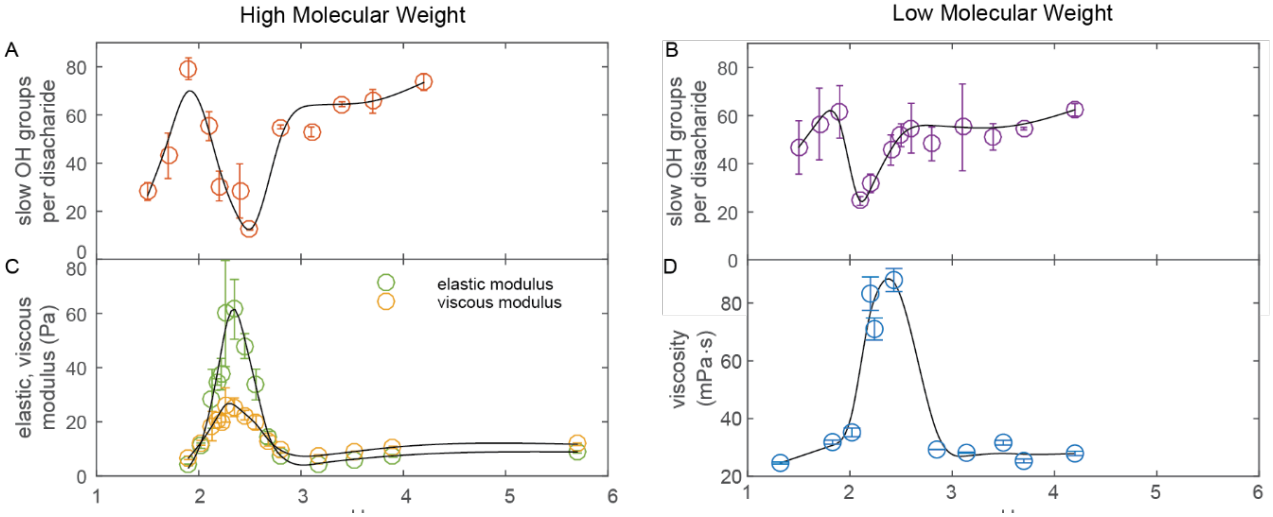

Figure 6. (A) Number of slow OH groups per disaccharide unit of the high molecular weight hyaluronan polymer as function of pH. (B) Number of slow OH groups per disaccharide unit of the low molecular weight hyaluronan polymer as function of pH. The number of slow OH groups per disaccharide unit is obtained after subtraction of the contribution of water molecules hydrating Na+, Cl- and ClO4- ions. (C) Elastic (green) and viscous (orange) modulus of 10 mg/ml high molecular weight hyaluronan solutions in water. (D) Viscosity 20 mg/ml of low molecular weight hyaluronan solutions in water. The solid lines are a guide to the eye.

in the elastic and viscous modulus is observed, reflecting the formation of the putty state. This finding agrees with previously reported rheology measurements.[13] For low-molecular weight hyaluronan, the rheological differences were too small to measure using conventional rheology as the molecular weight is too small for the chains to entangle and to form an elastic putty state. Therefore, we determined the viscosity of solutions of 20 mg/ml low molecular weight hyaluronan with differential dynamic microscopy (DDM), (Figure 6D).[23–25] For low-molecular weight hyaluronan we also observe a sharp increase of the viscosity around pH 2.4. Figure 6 shows that there exists a strong correlation of the macroscopic rheology and the changes in water dynamics probed by polarization-resolved pump-probe spectroscopy. The pH values at which we observe minima in the number of slow OH groups differ by less than 0.2 units from the pH values at which we observe the maxima in the viscosity. We thus arrive at the counterintuitive result that the strong increase in viscosity near pH 2.4 of aqueous hyaluronan solutions correlates to a substantial decrease of the fraction of slow water, i.e. an increase of the average orientational mobility of the water molecules. This change in interaction between water and hyaluronan is not visible from the pH dependent FTIR spectra of hyaluronic acid (see supplementary information and ref [16]), which can be explained from the fact that the hydrogen bonds that are formed by water molecules in the hydration shell of hyaluronic acid are similar in strength and number as the hydrogen bonds that are formed between water molecules in bulk liquid water. The change in local environment from hydration shell to bulk thus has little effect on the vibrational spectrum of the water molecules but obviously a strong effect on the orientational mobility. Femtosecond nonlinear infrared spectroscopy has as a unique capability that it can probe this change in molecular orientational mobility.

The observed reduction in number of slowed-down water implies that ~80% of the water molecules are being expelled from the polymer surfaces near pH 2.4. We ascribe this expulsion to the bundling of the polymer chains into fibres. Other research also suggests that the polymer chains bundle into fibres in the formation of the putty state.[16,26–29] The expulsion of water molecules during the formation of a connected network of fibers accounts both for the macroscopic observation of increased viscosity, and the molecular-scale observation of a decrease in slow water molecules interacting with the hyaluronic acid molecules. Interestingly, we observe the expulsion of water not only for high molecular weight hyaluronan, but also for low molecular weight hyaluronan that does not form a putty state.[21,22] This finding suggests that low-molecular weight hyaluronic polymer chains also form strong interchain connections near pH 2.4. However, in this case the polymer chains are not long enough to form a macroscopically connected network. As a result, low-molecular weight hyaluronan does not form an elastic putty state.

As shown in Figure 6, the number of slowly reorienting water hydroxyl groups also decreases when the pH is decreased from pH 1.9 to pH 1.5, both for high molecular weight and low molecular weight hyaluronan solutions. Lalevée and co-workers showed, using light scattering techniques, that at these very low pH values, the radius of gyration of hyaluronan decreases indicating a chain collapse.[30] Hence, also at these pH values water molecules get expelled, but not because of the formation of interchain connections (chain bundling) but because of the curling up of the individual hyaluronan chains.[16]

In an earlier femtosecond mid-infrared study by Hunger et al. of the properties of the solution state of hyaluronan at pH 7, it was found that 15±3 water molecules per disaccharide are affected in their reorientation dynamics.[31] This number is approximately 2 times smaller than the number of slow water molecules that we observe at pH 7. An important difference with this previous work is that we study solutions with a relatively low concentration of hyaluronan (20 mg/ml), while the measurements of Hunger et al. involved concentrations up to 200 mg/ml. At these high concentrations, saturation effects due to aggregation and sharing of hydration shells will occur, leading to a substantially lower number of slowed-down water molecules per hyaluronan disaccharide unit. In another femtosecond mid-infrared study hydration numbers of several monomeric sugar molecules were determined. In this study, a hydration number of 46±5 was found for the disaccharide trehalose.[32] This number is higher than the number of slowly reorienting waters of 33±5 (or 67±10 slow OH groups) per disaccharide unit that we find here for high-molecular weight hyaluronan in the solution state. This difference can be well explained from the fact that the disaccharide units of the hyaluronan polymer chains are in close proximity to each other, and that these chains will be somewhat folded, thus reducing the net amount of hydrating water molecules per disaccharide unit.

Conclusions

We studied the relation between the viscoelastic properties and the reorientation dynamics of water molecules for aqueous solutions of high-molecular weight and low-molecular weight hyaluronan. The viscoelastic properties are determined with rheology and differential dynamic microscopy (DDM), the water reorientation dynamics with polarization-resolved femtosecond mid-infrared pump-probe spectroscopy. We observe that the interaction between water and hyaluronan leads to a slowing down of the reorientation of a significant fraction of the water molecules.

We find both the viscosity and the reorientation dynamics to be strongly dependent on pH. For both low-and high-molecular weight hyaluronan the viscosity reaches a maximum near pH 2.4, while the number of slowed-down water molecules reaches a minimum. This finding implies that the water molecules show faster average reorientation dynamics when the solution is more viscous. This observation can be explained from the fact that around pH 2.4 hyaluronan the polymer chains bundle to form fibres, accompanied by expulsion of hydration water from the polymer chains.

For high-molecular weight hyaluronan, the expulsion of water and the bundling into fibers results in the formation of an elastic putty state. The reduction in number of slowed-down water shows that ~80% of the water molecules are being expelled

from the polymer surfaces in the formation of this state. For low-molecular weight the putty state is not observed. However, the molecular water reorientation dynamics show that the molecular-scale interactions between low-molecular weight hyaluronan and the water solvent are highly similar to those of high-molecular weight hyaluronan. For low-molecular weight hyaluronan likely no putty state is formed because the fibers formed near pH 2.4 are too short to form a macroscopically connected network. These results illustrate that the molecular-scale water dynamics can provide important additional information on the mechanism of macroscopic gelation in biopolymer solutions.

Conflicts of interest

There are no conflicts to declare.

Acknowledgements

We thank T. Sentjabrskaja for providing the Matlab program used in the analysis of the differential dynamic microscopy data. This work is part of the research program of the Netherlands Organization for Scientific Research (NWO) and of the Industrial Partnership Programme Hybrid Soft Materials that is carried out under an agreement between Unilever Research and Development B.V. and the Netherlands Organization for Scientific Research (NWO). The work was performed at the research institute AMOLF.

Notes and references

1 G. Kogan, L. Šoltés, R. Stern and P. Gemeiner, *Biotechnol. Lett.*, 2007, **29**, 17–25.
2 K. T. Dicker, L. A. Gurski, S. Pradhan-Bhatt, R. L. Witt, M. C. Farach-Carson and X. Jia, *Acta Biomater.*, 2014, **10**, 1558–1570.
3 A. Singh, M. Corvelli, S. A. Unterman, K. A. Wepasnick, P. McDonnell and J. H. Elisseeff, *Nat. Mater.*, 2014, **13**, 988–995.
4 A. G. OGSTON and J. E. STANIER, *J. Physiol.*, 1953, **119**, 244–52.
5 D. A. Swann, E. L. Radin, M. Nazimiec, P. A. Weisser, N. Curran and G. Lewinnek, *Ann. Rheum. Dis.*, 1974, **33**, 318–326.
6 X. Tian, J. Azpurua, C. Hine, A. Vaidya, M. Myakishev-Rempel, J. Ablaeva, Z. Mao, E. Nevo, V. Gorbunova and A. Seluanov, *Nature*, 2013, **499**, 346–349.
7 B. P. Toole, *Nat. Rev. Cancer*, 2004, **4**, 528–539.
8 B. P. Toole, *Semin. Cell Dev. Biol.*, 2001, **12**, 79–87.
9 M. F. Chaplin, *Proc. Nutr. Soc.*, 2003, **62**, 223–227.
10 R. Gyawali and S. A. Ibrahim, *Trends Food Sci. Technol.*, 2016, **56**, 61–76.
11 E. A. Balazs and J. Cui, *Bioact. Carbohydrates Diet. Fibre*, 2013, **2**, 143–151.
12 I. Gatej, M. Popa and M. Rinaudo, *Biomacromolecules*, 2005, **6**, 61–67.
13 S. Wu, L. Ai, J. Chen, J. Kang and S. W. Cui, *Carbohydr. Polym.*, 2013, **98**, 1677–1682.
14 A. B. Kayitmazer, A. F. Koksal and E. Kilic Iyilik, *Soft Matter*, 2015, **11**, 8605–8612.
15 D. A. Gibbs, E. W. Merrill, K. A. Smith and E. A. Balazs, *Biopolymers*, 1968, **6**, 777–791.
16 G. Giubertoni, F. Burla, C. Martinez-Torres, B. Dutta, G. Pletikapic, E. Pelan, Y. L. A. Rezus, G. H. Koenderink and H. J. Bakker, *J. Phys. Chem. B*, 2019, **123**, 3043–3049.
17 Y. L. A. Rezus and H. J. Bakker, *J. Chem. Phys.*, , DOI:10.1063/1.2009729.
18 T. Steinel, J. B. Asbury, J. Zheng and M. D. Fayer, *J. Phys. Chem. A*, 2004, **108**, 10957–10964.
19 Y. L. A. Rezus and H. J. Bakker, *Phys. Rev. Lett.*, 2007, **99**, 1–4.
20 S. T. Van Der Post, S. Scheidelaar and H. J. Bakker, *J. Phys. Chem. B*, 2013, **117**, 15101–15110.
21 E. A. Balazs, *Fed Proc*, 1966, **25**, 1817–1822.
22 O. Schmut and H. Hofmann, *Graefe's Arch. Clin. Exp. Ophthalmol.*, 1982, **218**, 311–314.
23 M. A. Escobedo-Sánchez, J. P. Segovia-Gutiérrez, A. B. Zuccolotto-Bernez, J. Hansen, C. C. Marciniak, K. Sachowsky, F. Platten and S. U. Egelhaaf, *Soft Matter*, 2018, **14**, 7016–7025.
24 P. Edera, D. Bergamini, V. Trappe, F. Giavazzi and R. Cerbino, *Phys. Rev. Mater.*, 2017, **1**, 073804.
25 A. V. Bayles, T. M. Squires and M. E. Helgeson, *Rheol. Acta*, 2017, **56**, 863–869.
26 B. Chakrabarti and E. A. Balazs, *J. Mol. Biol.*, 1973, **78**, 135–141.
27 J. K. Sheehan, K. H. Gardner and E. D. T. Atkins, *J. Mol. Biol.*, 1977, **117**, 113–135.
28 C. D. Blundell, P. L. Deangelis and A. Almond, *Biochem. J.*, 2006, **396**, 487–498.
29 P. GRIBBON, B. C. HENG and T. E. HARDINGHAM, *Biochem. J.*, 2000, **350**, 329.
30 G. Lalevée, L. David, A. Montembault, K. Blanchard, J. Meadows, S. Malaise, A. Crépet, I. Grillo, I. Morfin, T. Delair and G. Sudre, *Soft Matter*, 2017, 6594–6605.
31 J. Hunger, A. Bernecker, H. J. Bakker, M. Bonn and R. P. Richter, *Biophys. J.*, 2012, **103**, L10–L12.
32 C. C. M. Groot and H. J. Bakker, *Phys. Chem. Chem. Phys.*, 2015, **17**, 8449–8458.